Supplementary information

COVID-19 progression and convalescence in common variable immunodeficiency shows dysregulated adaptive immune responses and persistent type-I interferon and inflammasome activation

Supp. Figure 1

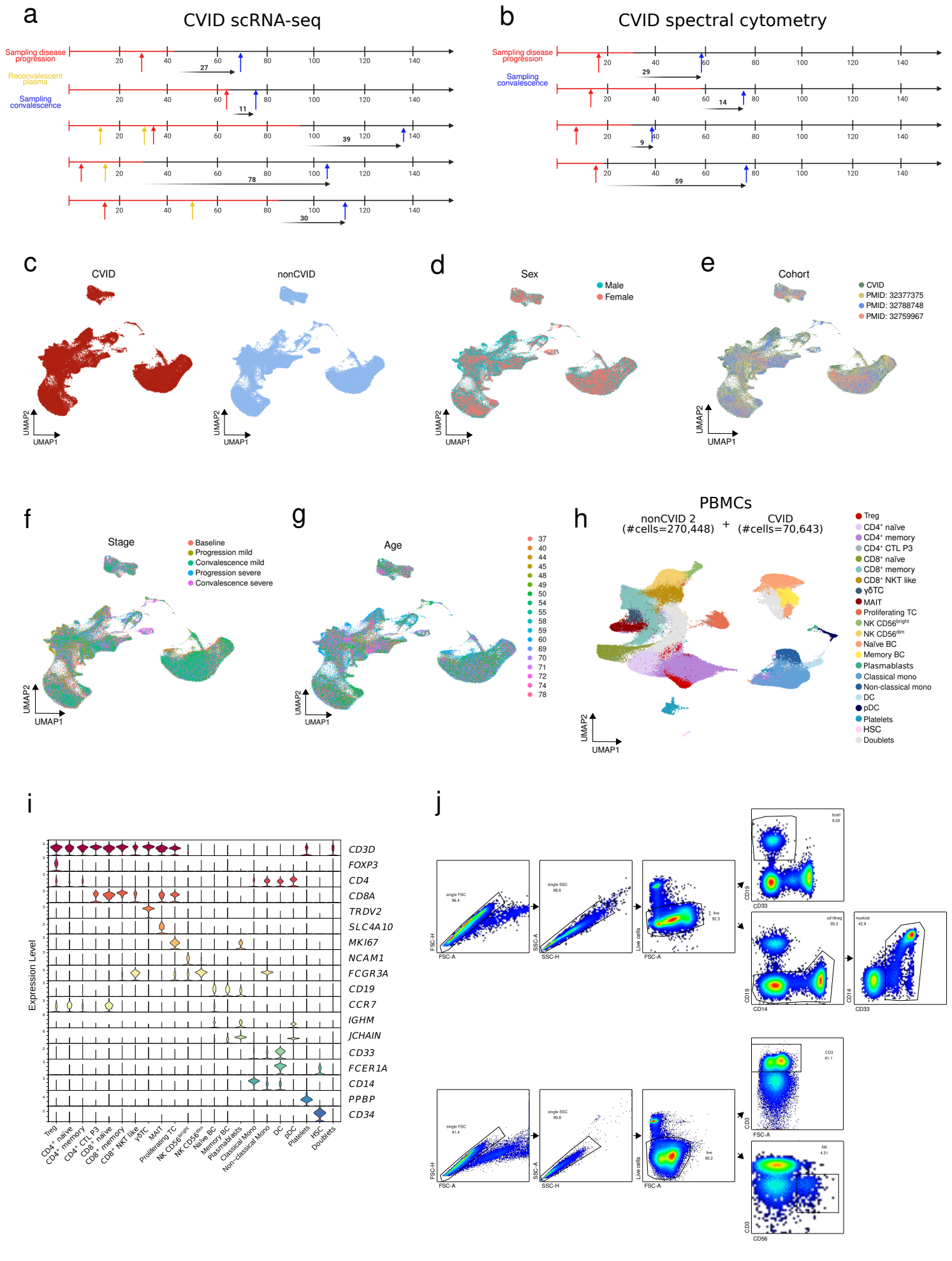

Supplementary Figure 1. (a) Overview of the CVID cohort analyzed by scRNA-seq. Red arrows indicate sample collection during progression, blue arrows during convalescence, yellow arrows for treatment with COVID-19 convalescent plasma, and black arrows for the time between negative PCR and convalescence sample collection. Red indicates positivity and black indicates convalescence. (b) Overview of the CVID cohort analyzed by spectral cytometry. Red arrows indicate sample collection during progression, blue arrows during convalescence, and black arrows for the time between negative PCR and convalescence sample collection. Red indicates positivity and black indicates convalescence. (c) UMAP visualizations of the CVID cohort and non-CVID1 cohort separately. (d) UMAP visualization of CVID + non-CVID1 cohorts colored by sex. (e) UMAP visualization of CVID + non-CVID1 cohorts colored by dataset. (f) UMAP visualization of CVID + non-CVID1 cohorts colored by SARS-CoV-2 infection stage and COVID-19 severity. (g) UMAP visualization of CVID + non-CVID1 cohorts colored by age. (h) UMAP visualization of non-CVID2 + CVID cohorts showing immune cell populations identified in Figure 1b. Non-CVID2 cohort: n=14 (baseline), n=11 (progression mild), n=8 (progression severe), n=8 (convalescence mild), n=5 (convalescence severe). CVID cohort: n=5 paired samples (baseline, progression, convalescence). Number of captured cells per cohort is in brackets. (i) Violin plots showing gene expression levels of selected markers in the non-CVID2 cohort. (j) Gating strategy used for spectral cytometry analysis. Source data for panels are provided in the Source Data Supp. Fig. 1 file.

Supp. Figure 2

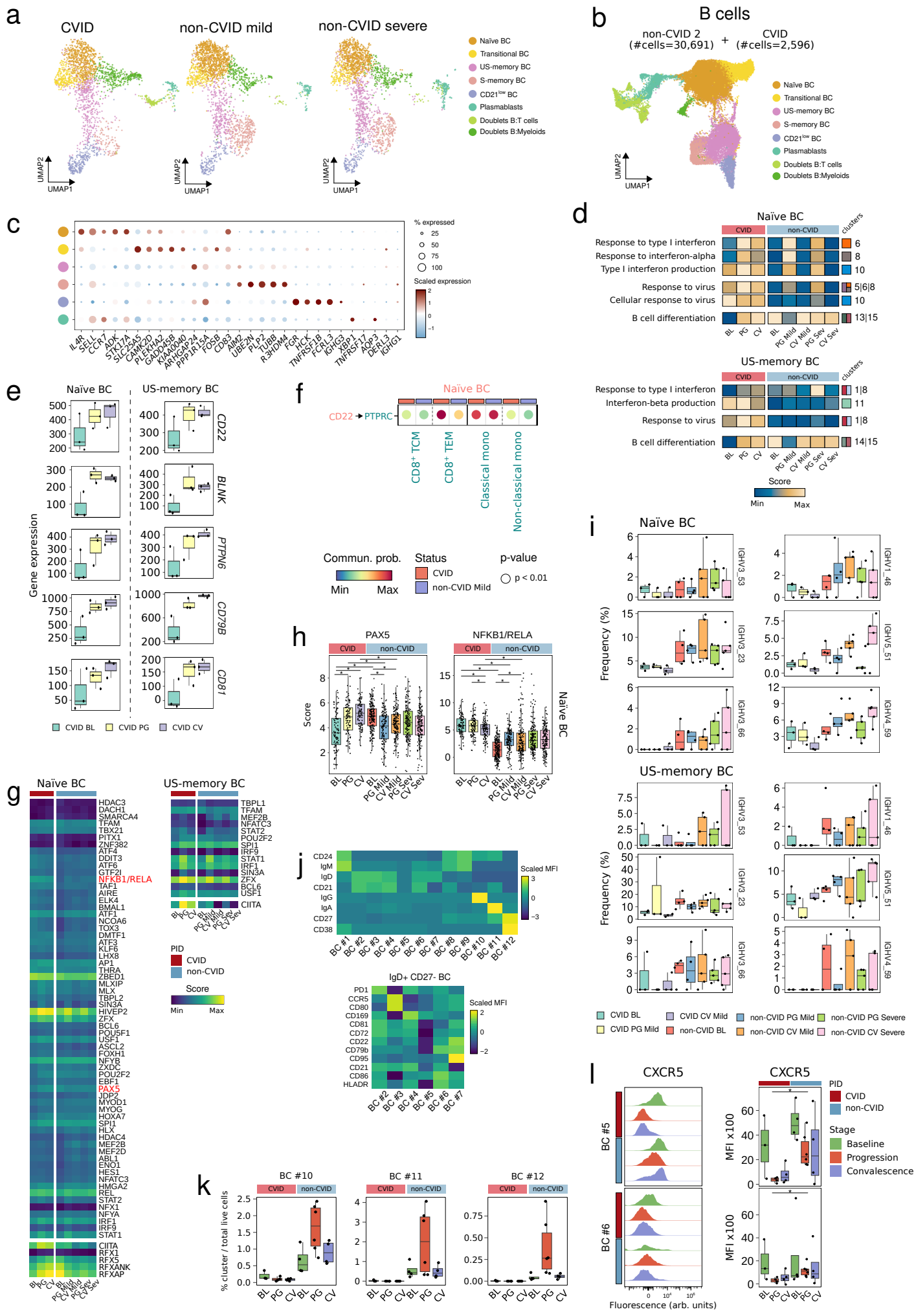

Supplementary Figure 2. (a) UMAP showing B cells in CVID and non-CVID1 cohorts, separated by PID status and COVID-19 severity. (b) UMAP of B cell subpopulations with cell numbers for CVID and non-CVID2 cohorts. (c) Dot plot showing expression of selected genes from Fig. 2b across CVID and non-CVID2 cohorts, with circle size indicating the percentage of expressing cells and colors representing scaled average expression. (d) Heatmap depicting score expression of selected GO categories shown in Figure 2d. (e) Box plots of BCR signaling pathway gene expression from CVID donors (CVID1, CVID2, CVID5) across infection stages. Dots represent biological replicates from different subjects in the CVID group (BL: n=3, PG: n=3, CV: n=3). (f) Cell-cell communication analysis of CD22 signaling during SARS-CoV-2 infection, showing sender cells and ligands (red), and receiver cells and receptors (green) with communication probability. (g) Heatmap of transcription factor (TF) activity. (h) Box plots of regulon activity for selected TFs. Two-sided Wilcoxon test was used (* p-value < 0.05). (i) Box plots of naïve and US-memory B cells expressing IGHV genes linked to SARS-CoV-2 neutralizing antibodies. Dots represent biological replicates from different subjects in the CVID (BL: n=3, PG: n=3, CV: n=3) and the non-CVID control group (BL: n=6, PG_Mild: n=4, CV_Mild: n=5, PG_Severe: n=5, CV_Severe: n=5). (j) Heatmap of protein markers used to annotate B cell clusters via spectral flow cytometry. (k) Box plot of IgA and IgG S-memory B cells and plasmablast frequencies in CVID and non-CVID samples during SARS-CoV-2 infection. (l) Histograms and box plots showing CXCR5 MFI in selected naïve B cell clusters. Dots represent biological replicates from different subjects in the CVID group (BL: n=3, PG: n=4, CV: n=4) and the non-CVID control group (BL: n=4, PG: n=6, CV: n=4). Two-sided t-test was used (* p-value < 0.05). BL: baseline, PG: progression, CV: convalescence. Source data for panels are provided in the Source Data Supp. Fig. 2 file.

Supp.Figure 3

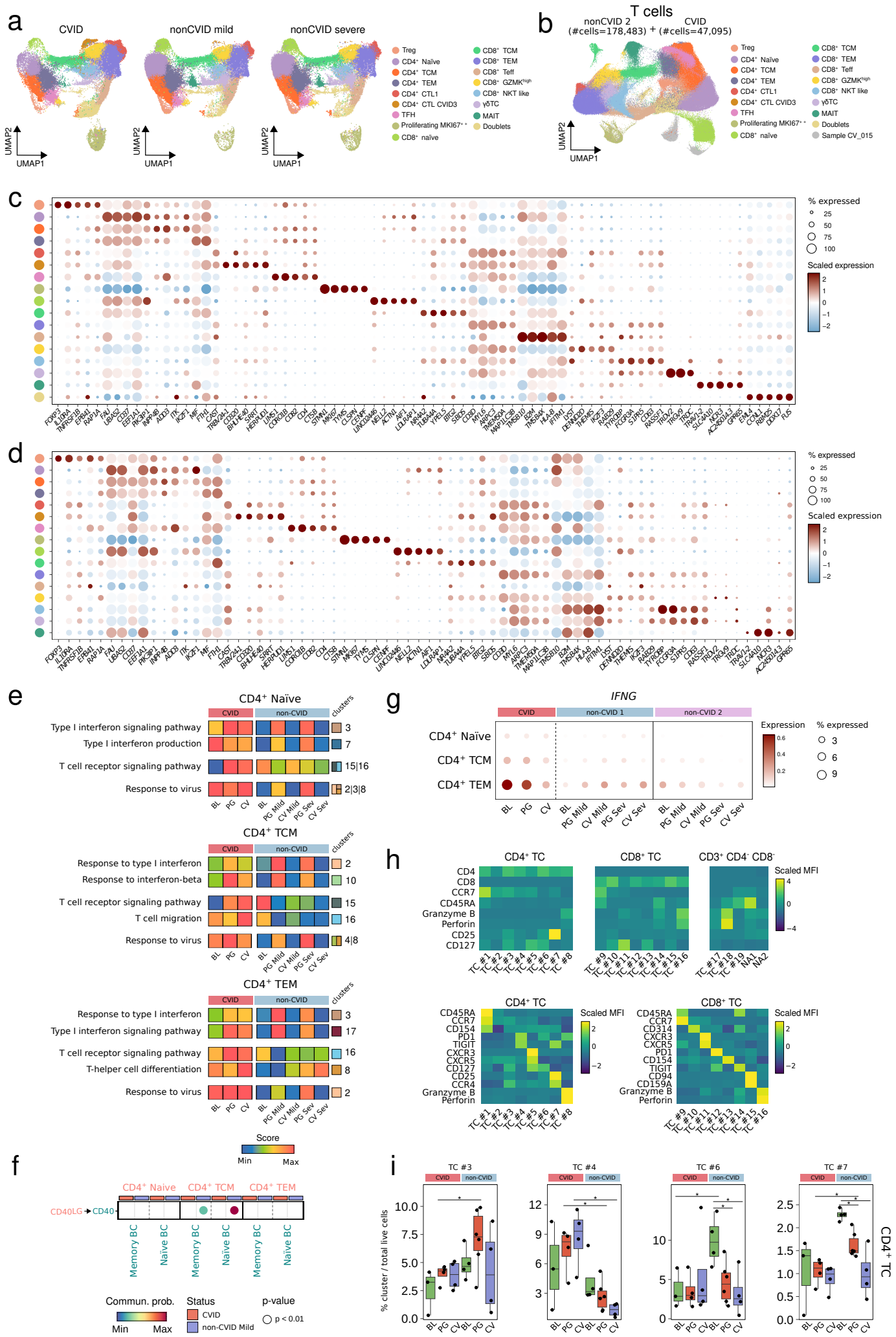

Supplementary Figure 3. (a) UMAP visualizations of the T cell compartment in the CVID and the non-CVID1 cohorts, split by PID and COVID-19 severity. (b) UMAP visualizations of the T cell compartment in CVID and non-CVID2 cohorts, with T cell numbers indicated in brackets. (c) Dot plot showing expression of specific genes in each T cell subset, where circle size represents the percentage of cells expressing the gene and colors indicate average expression levels. (d) Dot plot displaying expression of selected genes from Georg et al., used for T cell annotation in COVID-19 context; circle size indicates the percentage of expressing cells and colors represent scaled average expression. (e) Heatmap illustrating expression scores of GO categories in selected $CD4^+$ T cell subsets from CVID and non-CVID1 cohorts during SARS-CoV-2 infection. (f) Dot plot showing cell-cell communication analysis of CD40L/CD40 signaling pathway during SARS-CoV-2 infection, with sender cells/ligands in red and receiver cells/receptors in green. Scale indicates communication probability, and PID status and interaction significance are shown. (g) Dot plot showing expression of *IFNG* in selected $CD4^+$ T cell subsets; circle size indicates the percentage of expressing cells, and colors show average expression levels. (h) Heatmap presenting general markers for T cell clusters in spectral flow cytometry analysis. (i) Box plot displaying frequencies of selected $CD4^+$ T cell subsets in spectral flow cytometry analysis across CVID and non-CVID samples during SARS-CoV-2 infection. Dots represent biological replicates from different subjects in the CVID group (BL: n=3, PG: n=4, CV: n=4) and the non-CVID control group (BL: n=4, PG: n=6, CV: n=4). Two-sided t-test was used (* p-value < 0.05). BL: baseline, PG: progression, CV: convalescence. Source data for panels are provided in the Source Data Supp. Fig. 3 file.

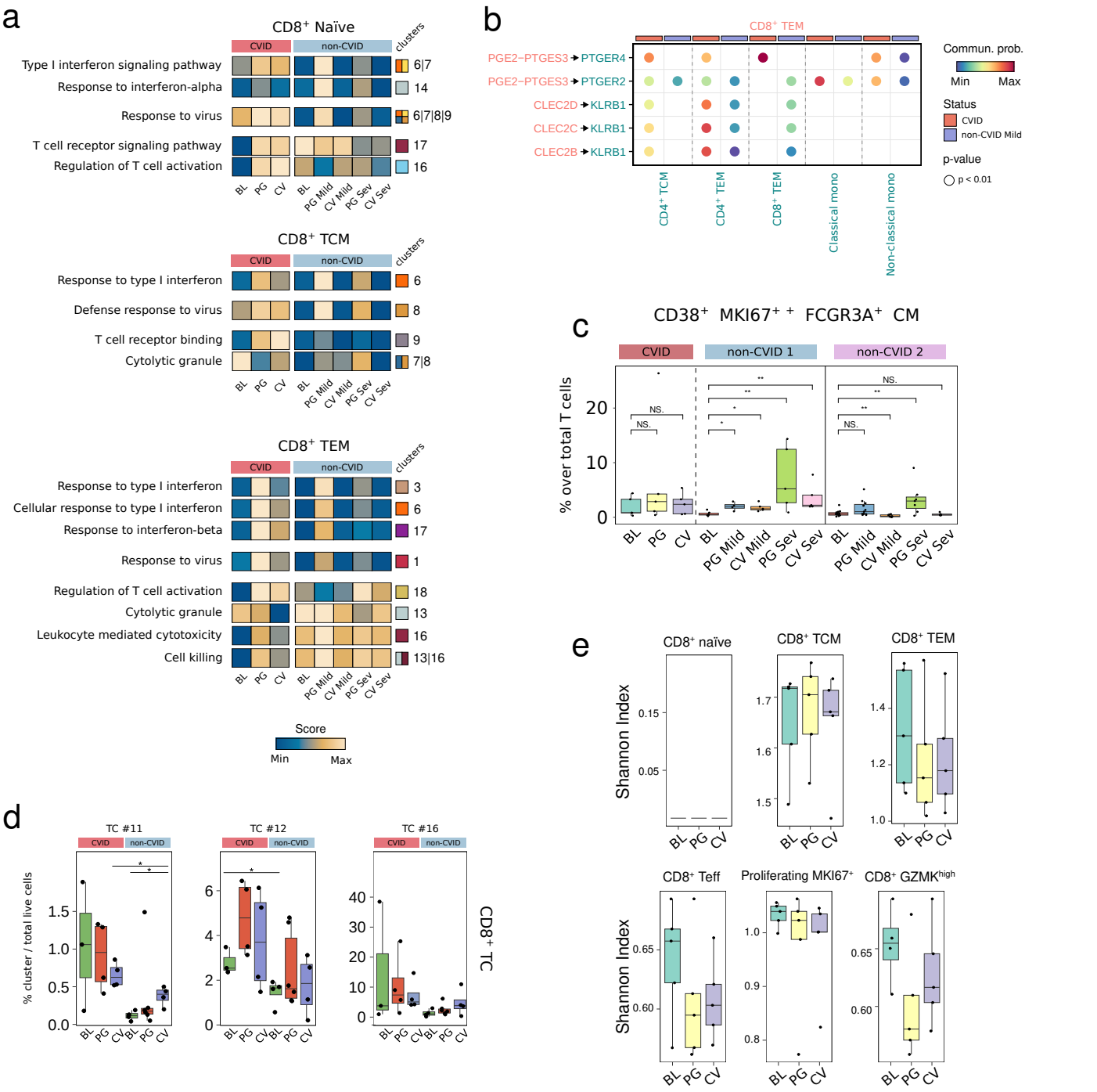
a
CD8+ Naïve
CVID
non-CVID
clusters
Type I interferon signaling pathway
Response to interferon-alpha
Response to virus
T cell receptor signaling pathway
Regulation of T cell activation
6|7
14
6|7|8|9
17
16
BL PG CV BL PG Mild CV Mild PG Sev CV Sev
CD8+ TCM
Response to type I interferon
Defense response to virus
T cell receptor binding
Cytolytic granule
6
8
9
7|8
CD8+ TEM
Response to type I interferon
Cellular response to type I interferon
Response to interferon-beta
Response to virus
Regulation of T cell activation
Cytolytic granule
Leukocyte mediated cytotoxicity
Cell killing
3
6
17
1
18
13
16
13|16
Score
Min
Max
b
CD8+ TEM
PGE2–PTGES3 → PTGER4
PGE2–PTGES3 → PTGER2
CLEC2D → KLRB1
CLEC2C → KLRB1
CLEC2B → KLRB1
CD4+ TCM
CD4+ TEM
CD8+ TEM
Classical mono
Non-classical mono
Commun. prob.
Min
Max
Status
CVID
non-CVID Mild
p-value
p < 0.01
c
CD38+ MKI67+ + FCGR3A+ CM
CVID
non-CVID 1
non-CVID 2
% over total T cells
NS.
BL PG CV BL PG Mild CV Mild PG Sev CV Sev
d
TC #11
TC #12
TC #16
CVID
non-CVID
% cluster / total live cells
CD8+ TC
e
CD8+ naïve
CD8+ TCM
CD8+ TEM
CD8+ Teff
Proliferating MKI67+
CD8+ GZMKhigh
Shannon Index
BL PG CV

Supplementary Figure 4. (a) Heatmap showing expression scores of selected GO categories in selected $CD8^+$ T cell subsets from CVID and non-CVID1 cohorts during SARS-CoV-2 infection. (b) Dot plot depicting cell-cell communication analysis of prostaglandin and CLEC signaling pathways during SARS-CoV-2 infection with sender cells/ligands indicated in red and receiver cells/receptors in green. Scale represents communication probability, with PID status and interaction significance shown. (c) Percentage of $CD38^+$ $MKI67^{++}$ $FCGR3A^+$ CM $CD8^+$ T cell subset (identified using Georg et al. annotation) across CVID, non-CVID1 and non-CVID2 cohorts, showing SARS-CoV-2 infection stage and COVID-19 severity. Two-sided wilcoxon test was used (* p-value < 0.05, ** p-value < 0.01). Dots correspond to biological replicates from different subjects in the CVID group (BL: n=5, PG: n=5, CV: n=5), the non-CVID1 control group (BL: n=6, PG_Mild: n=4, CV_Mild: n=5, PG_Severe: n=5, CV_Severe: n=5) and the non-CVID2 control group (BL: n=14, PG_Mild: n=11, CV_Mild: n=8, PG_Severe: n=8, CV_Severe: n=5). (d) Box plots displaying cell frequencies of selected $CD8^+$ T cell subsets observed in spectral flow cytometry analysis in CVID and non-CVID samples. Dots represent biological replicates from different subjects in the CVID group (BL: n=3, PG: n=4, CV: n=4) and the non-CVID control group (BL: n=4, PG: n=6, CV: n=4). Two-sided t-test was used (* p-value < 0.05). (e) Box plots illustrating Shannon index (diversity) of TCR clonality in different $CD8^+$ T cell clusters among CVID patients. Dots correspond to biological replicates from different subjects in the CVID group (BL: n=5, PG: n=5, CV: n=5). BL: baseline, PG: progression, CV: convalescence. Source data for panels are provided in the Source Data Supp. Fig. 4 file.

Supp.Figure 5

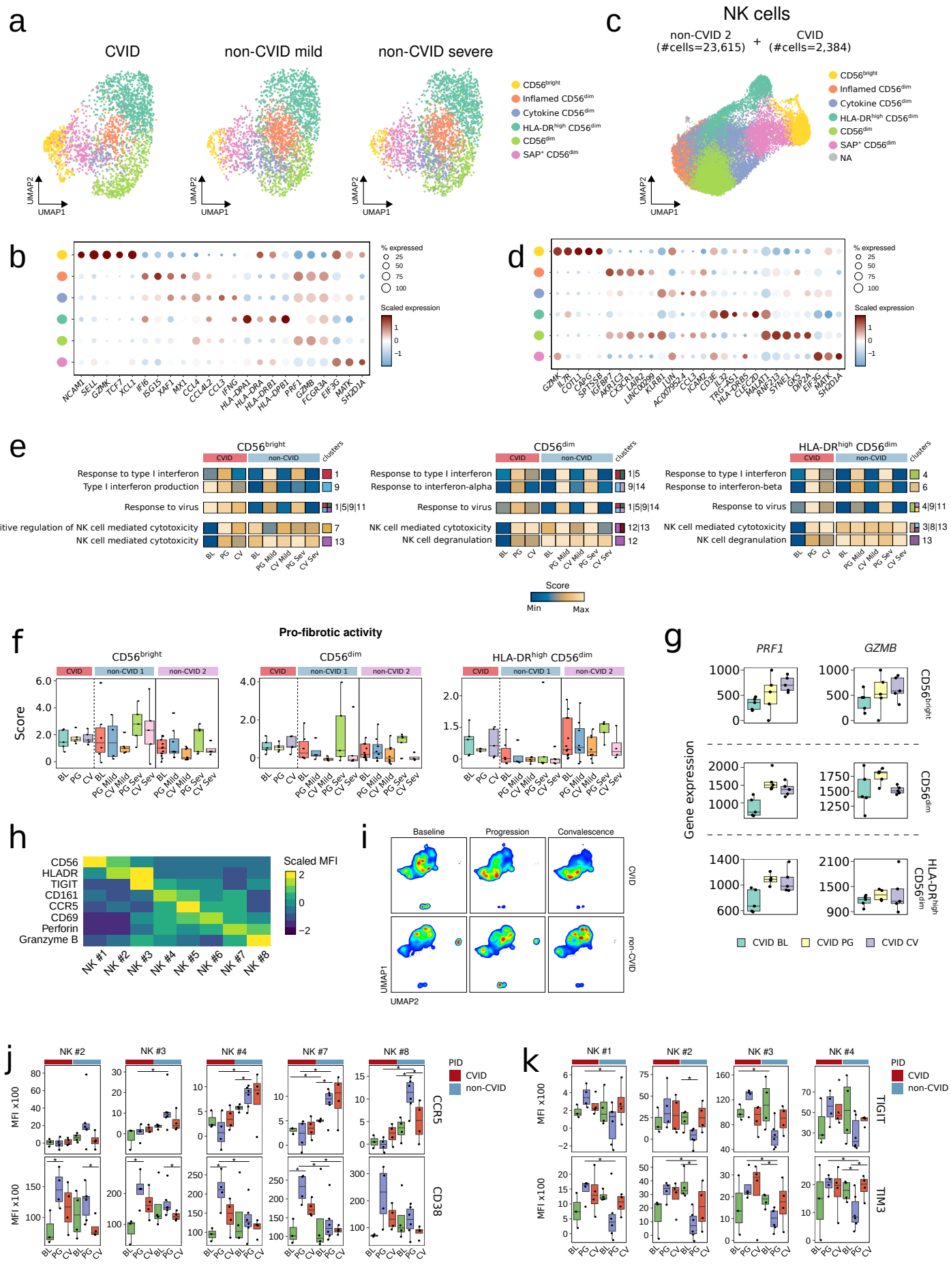

Supplementary Figure 5. (a) UMAP visualizations of NK cells in CVID and non-CVID1 cohorts, split by PID and COVID-19 severity. (b) Dot plot showing the expression of selected genes from Krämer et al.. Circle size indicates the percentage of cells expressing each gene with colors indicating the scaled average gene expression. (c) UMAP visualizations of NK cells in the CVID cohort and the non-CVID2 cohort, with the number of NK cells captured shown. (d) Dot plot showing the expression of selected genes from Figure 3b in CVID and non-CVID2 cohorts. Circle size indicates the percentage of expressing cells, with colors indicating scaled average expression. (e) Heatmap depicting score expression of selected GO categories shown in Figure 5d, in selected NK cell subsets from CVID and non-CVID1 cohorts. (f) Boxplot showing anti-fibrotic response in selected NK cell subsets in CVID, non-CVID1 and non-CVID2 cohorts. Dots correspond to biological replicates from different subjects in CVID group (BL: n=5, PG: n=5, CV: n=5), non-CVID1 control group (BL: n=6, PG_Mild: n=4, CV_Mild: n=5, PG_Severe: n=5, CV_Severe: n=5) and non-CVID2 control group (BL: n=14, PG_Mild: n=11, CV_Mild: n=8, PG_Severe: n=8, CV_Severe: n=5). (g) Box plots showing the expression of *PRF1* and *GZMB* in selected NK cell subsets from CVID donors. Dots correspond to biological replicates from different subjects in CVID group (BL: n=5, PG: n=5, CV: n=5). (h) Heatmap depicting markers used to annotate NK cell clusters in spectral flow cytometry analysis. (i) Density plots showing the distribution of NK cells. (j) Box plots showing the protein levels of CCR5 and CD38 in selected NK cell clusters. (k) Box plots showing the protein levels of TIGIT and TIM-3 in selected NK cell clusters. Panels j and k show biological replicates for CVID (BL: n=3, PG: n=4, CV: n=4) and non-CVID controls (BL: n=4, PG: n=6, CV: n=4). Two-sided t-tests were used (* p-value < 0.05). BL: baseline, PG: progression, CV: convalescence. Source data for panels are provided in the Source Data Supp. Fig. 5 file.

Supp.Figure 6

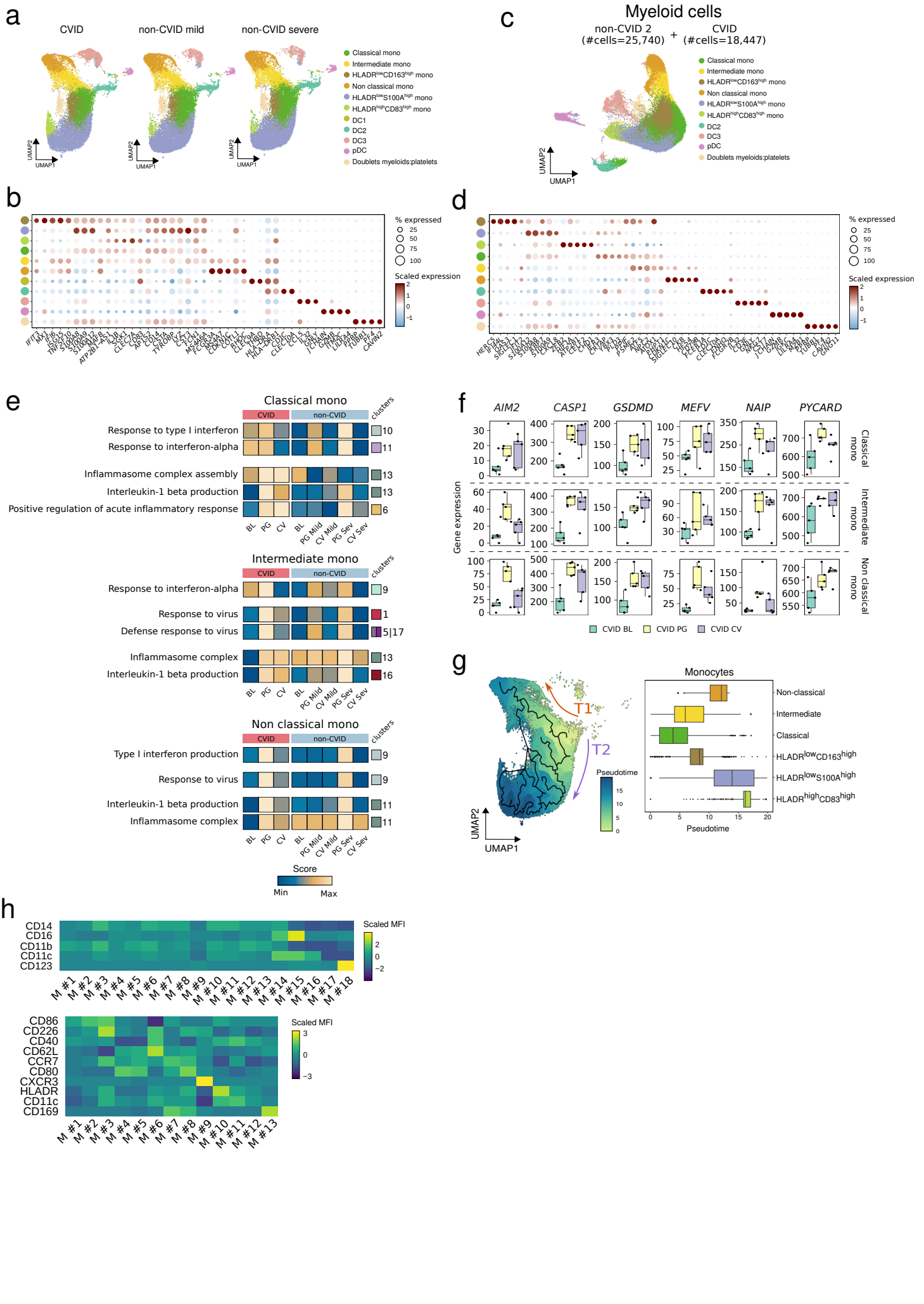

Supplementary Figure 6. (a) UMAP visualizations of the myeloid cell compartment in CVID and in non-CVID1 cohorts, split by PID and COVID-19 severity. (b) Dot plot showing the expression of selected genes from Schulte-Schrepping et al., used to annotate myeloid cells in the context of COVID-19. Circle size indicates the percentage of cells expressing the indicated gene, with colors representing scaled average expression. (c) UMAP visualizations of the myeloid cell compartment in CVID and in non-CVID2 cohorts, with the number of captured myeloid cells shown in brackets. (d) Dot plot showing the expression of selected genes from Figure 6c in CVID and non-CVID2 cohorts, with circle size reflecting the percentage of cells expressing each gene and colors indicating scaled average expression. (e) Heatmap depicting score expression of selected GO categories shown in Figure 6e, in selected monocyte subsets from CVID and non-CVID1 cohorts during SARS-CoV-2 infection. (f) Box plots showing the expression of selected inflammasome-related genes in selected monocyte subsets from CVID samples along SARS-CoV-2 infection. Dots correspond to biological replicates from different subjects in the CVID group (BL: n=5, PG: n=5, CV: n=5). (g) UMAP visualization and box plots showing cell trajectory in the myeloid cell compartment. UMAP scale refers to trajectory pseudotime. The trajectory seed was set in classical monocytes and two alternative trajectories were defined: trajectory 1 (T1) and trajectory 2 (T2). (h) Heatmap depicting general markers used to annotate myeloid cell clusters (top) or classical monocytes (bottom) in spectral flow cytometry analysis. BL: baseline, PG: progression, CV: convalescence. Source data for panels are provided in the Source Data Supp. Fig. 6 file.

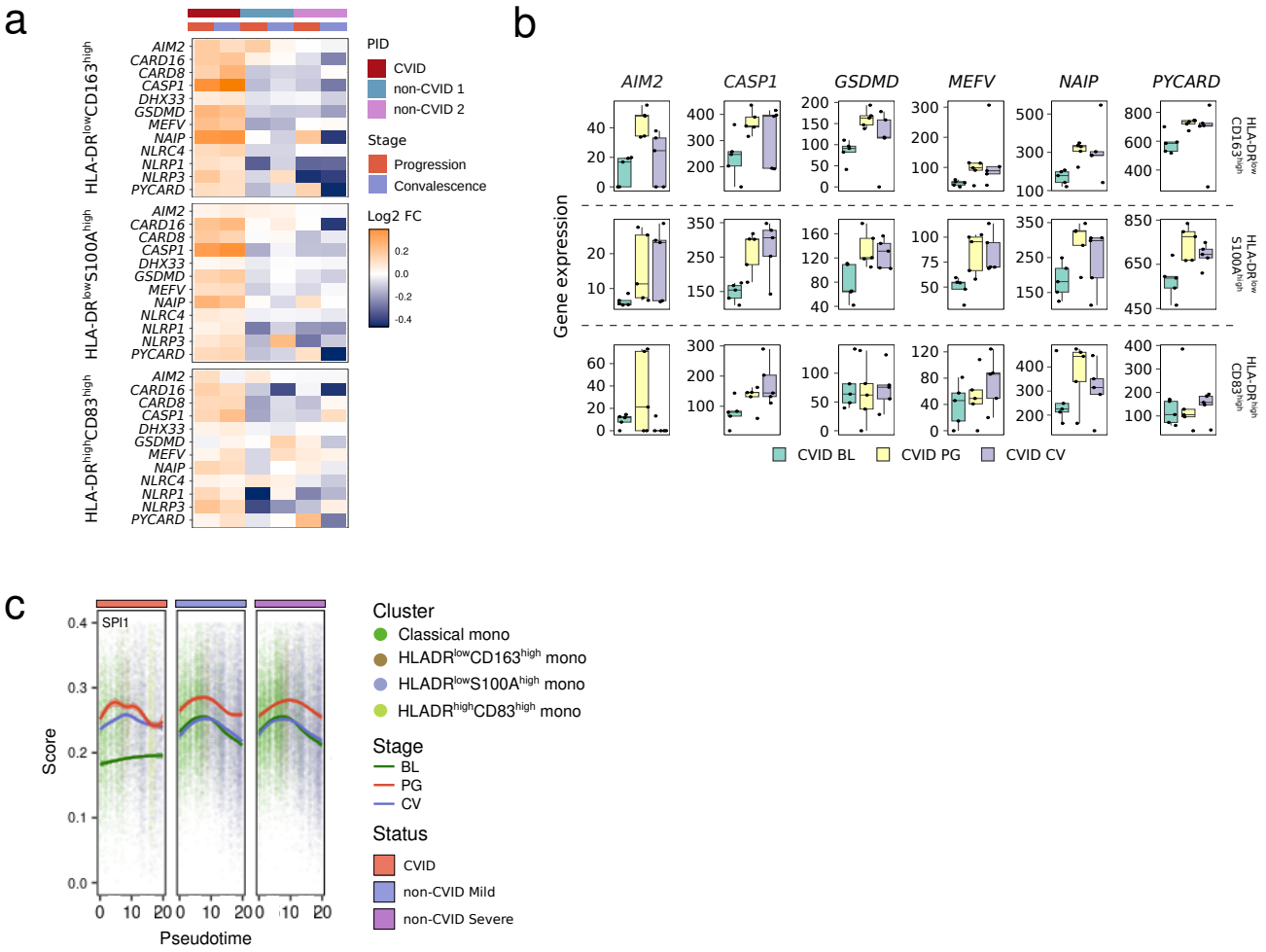
a
HLA-DR^low CD163^high
HLA-DR^low S100A^high
HLA-DR^high CD83^high
AIM2
CARD16
CARD8
CASP1
DHX33
GSDMD
MEFV
NAIP
NLRC4
NLRP1
NLRP3
PYCARD
PID
CVID
non-CVID 1
non-CVID 2
Stage
Progression
Convalescence
Log2 FC
0.2
0.0
-0.2
-0.4
b
AIM2
CASP1
GSDMD
MEFV
NAIP
PYCARD
Gene expression
CVID BL
CVID PG
CVID CV
c
SPI1
Score
Pseudotime
Cluster
Classical mono
HLADR^low CD163^high mono
HLADR^low S100A^high mono
HLADR^high CD83^high mono
Stage
BL
PG
CV
Status
CVID
non-CVID Mild
non-CVID Severe

Supplementary Figure 7. (a) Heatmaps showing the fold change (baseline versus progression or convalescence) of selected inflammasome-related genes in selected myeloid subsets from CVID, non-CVID1 and non-CVID2 cohorts. Only COVID-19 mild samples are shown. PID status and SARS-CoV-2 infection stage are indicated. Scale color indicates the Log2(fold change). (b) Box plots showing the expression of selected inflammasome-related genes in selected myeloid subsets from CVID donors along SARS-CoV-2 infection. Dots correspond to biological replicates from different subjects in the CVID group (BL: n=5, PG: n=5, CV: n=5). (c) Plots representing the score of genes regulated by the transcription factor PU.1 (SPI1) at the single-cell level and ordered by pseudotime in the trajectory 2 of the myeloid cell compartment (Supp. Figure 6g). Myeloid cell subset, SARS-CoV-2 infection stage, PID status and COVID-19 severity are shown. BL: baseline, PG: progression, CV: convalescence. Source data for panels are provided in the Source Data Supp. Fig. 7 file.